PAPER

Check for updates

CO$_2$ free production of ethylene oxide *via* liquid phase epoxidation of ethylene using niobium oxide incorporated mesoporous silica material as the catalyst†

Muhammad Maqbool,[a] Toheed Akhter, [ID] *[a] Muhammad Faheem,[a] Sohail Nadeem,[a] Chan Ho Park*[b] and Asif Mahmood*[c]

Ethylene Oxide (EO) is an essential raw material used in various consumer products like different glycol derivatives, ethoxylates, and polymers. We hydrothermally synthesize niobium oxide incorporated with mesoporous silica material (Nb/MSM), an efficient catalyst for CO$_2$ free-ethylene oxide (EO) production *via* partial oxidation of ethylene. The structural properties of Nb/MSM catalysts were characterized using XRD, TEM, and N$_2$ adsorption–desorption. The catalytic activity of synthesized materials in liquid phase epoxidation (LPE) of ethylene was evaluated in the presence of peracetic acid (PAA) as an oxidant to avoid the production of CO$_2$ and also minimize metal leaching. GC chromatography was used to investigate the successful production of EO, and a peak with a retention time (RT) of 9.01 min served as confirmation. Various reaction parameters *viz.* temperature, catalyst concentration, ethylene to PAA molar ratio, and solvent effect were investigated in order to optimize the reaction conditions for enhancing the ethylene conversion and selectivity for EO production. By this approach, the challenges of greenhouse gas production and metal leaching were addressed which were associated with previously reported catalysts.

1. Introduction

In the field of epoxidation, various materials have been explored to assess their potential as efficient catalysts for polyethylene, polyvinyl chloride, and ethylene oxide (EO) production. In particular, EO is the third-largest ethylene derivative which is used as raw/starting material for the synthesis of a wide range of commodities.[1] The traditional method of producing EO is to use oxygen (O$_2$) as an oxidant at a temperature of 392–500 °F under a pressure of 10–30 bar in the presence of a silver-based catalyst.[2,3] However, the epoxidation reaction's selectivity is very poor (around 85%) in this method leading to the production of a huge amount of CO$_2$ as a by-product making it the second-highest emitter of CO$_2$ as a by-product among all chemical processes after ammonia synthesis.[2,3] Researchers have tried to change the CO$_2$-emitting gas-phase epoxidation (GPE) to a CO$_2$-free liquid-phase epoxidation (LPE).[3] The LPE employs

a homogeneous methyltrioxorhenium (MTO) catalyst and H$_2$O$_2$ as an oxidant, resulting in a high catalytic performance with nearly 100% EO selectivity.[4] However, there are two disadvantages of MTO used in this method: (1) the catalyst is deactivated by the accumulation of water (as a by-product); (2) the cost of Re metal is high, and its supply is unstable. Thus, using less expensive catalytic materials with high H$_2$O$_2$ usage efficiency instead of Re could increase process economics and practical possibilities.[5] As a result, further research should be carried out to develop a different heterogeneous epoxidation catalyst.[6]

In this quest, previous studies have paid attention to the catalysts consisting of transition metals in high oxidation states supported on mesoporous silica material (MSM), specifically MCM-41 and SBA-15.[7–11] It was observed that the substrate was catalyzed *via* the redox reaction by facilitating oxygen transfer from oxidant to alkene double bond.[12–16] Among the various metals for the efficient catalyst, niobium (Nb)-based catalysts have been shown significant catalytic activity in the epoxidation of cyclic alkenes, propene, and other chemical substrates such as carvone and limonene with excellent thermal stability and resistance to metal leaching and hydrolysis suitable for LPE process.[17–25] A combination of Nb/MSM has been reported by using Nb/MCM-41 and MCM-48 during the oxidation of cyclohexene. Nevertheless, only at low incorporation of Nb metal into MCM-48 support shown efficient selectivity of

[a] Department of Chemistry, University of Management and Technology, C-II, Johar Town, Lahore, 54770, Pakistan. E-mail: Toheed.akhter@umt.edu.pk

[b] Department of Chemical and Biological Engineering, Gachon University, Seongnam, 13120, Republic of Korea. E-mail: chhopark@gachon.ac.kr

[c] College of Engineering, Department of Chemical Engineering, King Saud University, 11421 Riyadh, Saudi Arabia. E-mail: ahayat@ksu.edu.sa

epoxidation.[17,26-31] Also, there has been rarely reported about the Nb/MSM-based EO production: Yan *et al.* studied tungsten (W) and Nb based MSM as ethylene epoxidation catalysts with H_2O_2 as the oxidant.[32] It was observed that both W-KIT-6 and Nb-KIT-6 metals catalysts are efficient for the production of EO under normal conditions. However, significant metal leaching and H_2O_2 decomposition was the main drawback associated with W-KIT-6, and Nb-KIT-6-based catalysts.[33]

Here, we have developed an EO production method with zero greenhouse gas emission. For this purpose, Nb/MSM hetero-catalyst was used along with peracetic acid (PAA) as an oxidant. This catalyst was prepared *via* a hydrothermal procedure in which $NbCl_5$ was used to incorporate Nb metal into ordered cubic large pore mesoporous silicate (SiO_2) which was generated from TEOS. The PAA was chosen as an oxidant because it reacts with ethylene gas to produce EO along with by-products such as acetic acid (AA), ethylene glycol (EG), and its derivatives. These by-products are also quite significant and have their own applications in different fields.

The heteroatom structure of Nb/MSM was confirmed by XRD analysis while the porosity was also investigated by BET analysis. The morphology of the catalyst was evaluated by TEM. The prepared catalyst was used for EO production *via* liquid phase epoxidation process in which the ethylene gas was compressed (under pressure, 50 bars) and dissolved in a liquid reaction medium of PAA. This LPE process was used for the production of EO and acetic acid which was confirmed by gas chromatography (GC). The GC analysis confirmed that the conversion of ethylene to EO was 79.5% and selectivity was found to be 84.3%. Thus, in this whole process, highly desirable EO was produced along with useful by-products with zero emission of CO_2 making it an environment-friendly method of EO production.

2. Experimental

2.1 Materials

Tetraethylorthosilicate (TEOS) (Sigma-Aldrich, Germany 98%), Pluronic P123 (Sigma-Aldrich, Germany), niobium(v) chloride (Sigma-Aldrich, Germany), sodium thiosulphate (Sigma-Aldrich, Germany), concentrated sulphuric acid (Merck, Germany), 1-ethanol (Sigma-Aldrich, Germany), peracetic acid 32% (Sigma-Aldrich, Germany), and distilled water. All the chemicals and reagents were used as received without any further purification.

2.2 Synthesis of catalyst (Nb/MSM)

For the synthesis of the Nb/MSM, 6.0 g of Pluronic P123 was dissolved in a solvent mixture containing 218 mL of distilled water and 7.92 mL of 35% conc. HCl at 35 °C. After complete dissolution, 7.41 mL of *n*-butanol was added to this solution with continuous stirring at 35 °C over 1 hour. Then, 1.539 g of $NbCl_5$ and TEOS (14.849 mL) was poured into this solution dropwise under the same conditions. The resulting mixture was stirred for 24 h at 35 °C and then heated at 100 °C for the next 24 h in a closed flask (hydrothermal process), which resulted in the formation of precipitates in the reaction mixture.[39] These

precipitates were filtered off and dried at 100 °C overnight. Then, the crude product was washed with a mixture of ethanol and HCl (1 : 1). The purified product was then calcined at 550 °C for 5 hours leading to the preparation of MSM which was the support of the catalyst.

2.3 Synthesis of the MSM

For the evaluation of the properties, MSM (support of the catalyst) alone was prepared using the same synthesis procedure of Nb/MSM, except $NbCl_5$ was not added to the reaction mixture with TEOS.
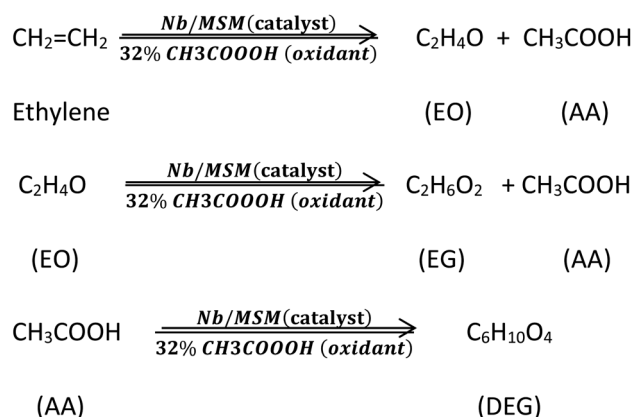
2.4 EO production

The synthesized catalyst was used for the production of ethylene oxide *via* liquid-phase epoxidation of ethylene as shown in Fig. S1.† The peracetic acid, acetonitrile, and catalyst were added to the reactor. Subsequently, pure ethylene gas was introduced from a cylinder. The consumption of ethylene gas was monitored by a weighing balance. The pressure in the reactor was controlled by the pressure controller mounted on the tail of the gas line. The reactor temperature was controlled using an oil bath (temperature range = −20 to 200 °C) equipped with a digital heater, cooler, and a variable speed pump. The reaction was carried out under different sets of parameters, including temperature (40 °C, 50 °C, and 60 °C) and reaction time (1 h, 2 h, 3 h, 4 h, 5 h, and 6 h). In all these conditions, the pressure was kept constant at 50 bars.

At the end of each experiment, a certain amount of the sample was taken and injected to GC. As a reference, all these experiments were also carried out using prepared MSM alone instead of the NB/MSM.

The reaction procedures are also shown in Scheme 1.

The concentration of produced EO, and EO selectivity was calculated by given equations.

$$\text{Conc. of target compound} = \frac{\text{conc. of std. sample}}{\text{peak area of std. sample}}$$
$$\times \text{peak area of target compound} \qquad (1)$$

Scheme 1 Production of EO and its derivatives from ethylene.

EO selectivity

$$= \frac{\text{amount of EO formed}}{\text{total amount of all possible reaction products}} \times 100 \quad (2)$$

The utilization (U_{PAA}) and conversion (X_{PAA}) efficiencies of PAA were calculated by a reported method.[34]

$$U_{PAA} = (\eta_{EO} + \eta_{MEG} + \eta_{DEG}/\mathring{\eta}_{PAA} - \eta_{PAA}) \times 100\%$$

$$X_{PAA} = \mathring{\eta}_{PAA} - \eta_{PAA}/\mathring{\eta}_{PAA} \times 100\%$$

η_{EO}, η_{MEG}, η_{DEG} = moles of EO, monoethylene glycol (MEG), and diethylene glycol (DEG), respectively. $\mathring{\eta}_{PAA}$ and η_{PAA} = initial and final moles of PAA.

3. Characterization

The formation of the support (MSM) and the catalyst (Nb/MSM) was confirmed by Miniflex Benchtop powder X-ray diffractometer (Rigaku, Japan) with Cu Kα irradiation ($\lambda = 1.5418$ Å, 200 kV, 50 mA) in the range of $2\theta = 2°$ and $8°$ for the support and $10°–80°$ for the catalyst Nb/MSM. The average size of crystallites (size error 0.5 nm) was calculated from the XRD diffractogram using Scherrer equation.[35,36] The surface area of the support and catalyst was measured *via* N$_2$ adsorption–desorption process using Micro-metrics Gemini VII 2390t Automated Gas Sorption Instrument at 77 K and a pressure range of 0.05–0.30 bars. The Brunauer–Emmett–Teller (BET) technique was used to determine the pore size distributions of the samples based on the desorption values. Prior to analysis, the samples were heated at 150 K under a vacuum for 4 h.[37] TEM microscope (JEOL 2010F) was used for obtaining TEM images at a higher resolution, working with a high voltage of 200 kV. The samples for the TEM analysis were prepared using a suspension of samples, which was diluted with methanol and then drop-dried on the holey carbon-coated copper TEM grids. Gas chromatography was carried out using Agilent GC-7890A equipped with GC Column DB-WAX capillary column (30 μm, 320 μm, 0.25 μm).

4. Results and discussion

The successful synthesis of the catalyst and its support was confirmed by XRD analysis and their diffractograms are shown in Fig. 1. In the XRD pattern of MSM (Fig. 1a), a single broad peak is present at $2\theta = 1.7°$ which exhibits that MSM is completely amorphous after calcination at 550 °C for 5 h. In the case of Nb/MSM (Fig. 1b), the XRD diffractogram is of a typical mesoporous silica material with a broad peak at $2\theta = 26.5°$ in XRD pattern that can be attributed to Nb$_2$O$_5$. This result suggests that Nb ions are well bonded and uniformly distributed on the inner and outer channels of MSM without any changes in the amorphous nature of the MSM framework. These results are in good agreement with previously published literature.[38]

The surface property of Nb/MSM and MSM was analyzed by BET analysis at 77 K. According to IUPAC Nomenclature, Nb/MSM and MSM can be classified as type IV isotherm as shown
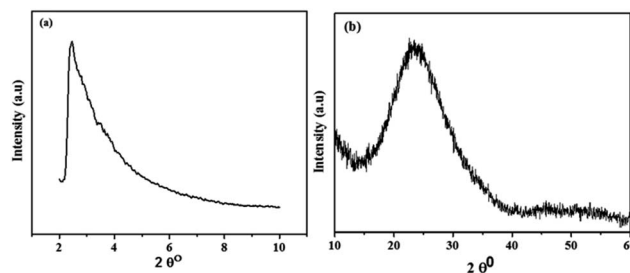

Fig. 1 Low-angle and wide-angle X-ray diffraction (a) of MSM and (b) of Nb/MSM.

Fig. 2 (a) Pore size distribution (b) N$_2$ adsorption–desorption isotherm.

in Fig. 2. The hysteresis loops show that these isotherms are characteristic of highly organized mesoporous silica materials. The support MSM has a large surface area of 270.48 m^2 g^{-1} and a pore volume of 0.434 cm^3 g^{-1}. After loading of Nb metal on MSM, the significant reduction in the surface area was observed from 270.475 to 129.400 m^2 g^{-1}. Also, the pore volume was decreased from 0.434 to 0.163 cm^3 g^{-1} which indicates the partial blockage of mesoporous silica material as shown in Fig. 2b. The pore size distribution of Nb/MSM and MSM was estimated by Barrett–Joyner–Halenda (BJH) method.[39,40] Furthermore, the capillary condensation of Nb/MSM and MSM was also measured from the adsorption–desorption curve (Fig. 2b) to assess the uniformity of the pore size. This capillary condensation of nitrogen within the pores is primarily responsible for detecting the sharp inflection at a relative pressure (p/p^0) between 0.5 and 0.7. The degree of uniformity of pore size is determined by the height and sharpness of the inflection. It was observed that the average pore diameter has a value of 4.54 nm in the case of Nb/MSM, while MSM has a pore diameter of 4.15 nm. These results are comparable to previous literature.[41,42] In BET analysis, surface area (S_{BET}), cumulative pore volume (V_{BJH}), and mesoporous diameter (D_{BJH}) are among the textural parameters listed in Table 1.

Table 1 BET analysis of Nb/MSM and MSM

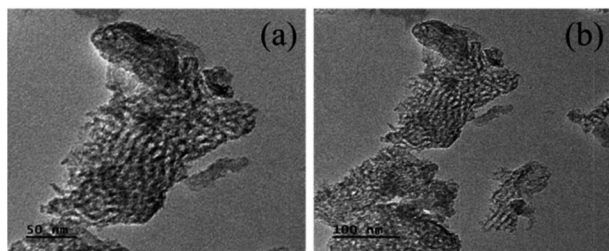| Entry	Material	S_{BET} (m^2 g^{-1})	V_{BJH} (mL g^{-1})	(D_{BJH}) (nm)
1	MSM support	270.475	0.434	4.152
2	Nb/MSM	129.400	0.163	4.543

Fig. 3 TEM images of Nb/MSM catalyst.

The porous nature and morphology of the Nb/MSM catalyst was evaluated by TEM and micrographs at a resolution of 50 and 100 nm are shown in Fig. 3. These TEM images confirm the mesoporous structure of the Nb/MSM. It can be observed from the TEM images that Nb_2O_5 nanoparticles, having a size of 20–30 nm, are well dispersed in the MSM support. It shows that the incorporation of Nb_2O_5 nanoparticles into MSM support does not damage the geometry of the silica framework.[27] This fact was also exhibited by XRD and BET analysis.

4.1 Catalytic activity

4.1.1 Epoxidation of ethylene using Nb/MSM catalyst. Epoxidation of ethylene was performed in the presence of peracetic acid (PAA) as an oxidant and Nb/MSM heterocatalyst. Similarly, as a control experiment, this epoxidation was carried out in the presence of PAA and MSM support without Nb/MSM catalyst.[43] In the typical procedure, a reaction mixture containing 3.28 mmol of ethylene, 5.5 mmol of PAA, 0.3 g of Nb/MSM catalyst, and 20 mL of acetonitrile (C_2H_3N) was heated at 40 °C for a period of 6 h, which resulted in the production of EO. The successful production of EO was confirmed by GC analysis and GC chromatograms are presented in Fig. 4. As it is obvious from the GC chromatogram in Fig. 4a, a peak at a retention time of 9.01 min can be associated to EO confirming the production of EO in the process. The peaks at a retention time of 23.6, 27.2, and 31.2 min correspond to the acetic acid, monoethylene glycol, and diethylene glycol as the valuable by-products of our LPE method. It is also evident from the GC analysis that no peak is present at the retention time of 3.5 min (Fig. 4a) confirming that no CO_2 was produced in the presented procedure making it an environment friendly method of EO production. Whereas, no EO and by-products were produced in the control experiment where MSM support was used instead of Nb/MSM to catalyze EO production as shown in Fig. 4b. Furthermore, the Nb/MSM catalyst showed an excellent selectivity of 90.1% towards EO production with a mild conversion (57%) of ethylene to EO (Fig. 4c).

Data derived from epoxidation of ethylene using Nb/MSM, MSM and a blank is presented in Table 2. As obvious from the data, 14.3% conversion efficiency and 17.21% utilization efficiency of PAA was achieved using Nb/MSM catalyst.

When MSM was used instead of Nb/MSM, no decomposition of PAA was observed and also no EO was produced. Whereas in the blank run a conversion efficiency of PAA of 11.4% was noted. In the blank run, the decomposition of PAA can be

Fig. 4 GC chromatogram of (a) Nb/MSM, (b) MSM support and (c) ethylene conversion and selectivity of Nb/MSM towards EO production [reaction condition: ethylene = 3.28 mmol, (32%) PAA = 5.5 mmol, temperature = (50 °C), amount of catalyst (10 wt%) = 0.3 g, solvent = C_2H_3N (20 mL), time = 6 h].

attributed to the acidity of the catalyst caused by the incorporation of Nb into MSM which is in good agreement to previously published literature.[32]

Furthermore, TOF of Nb/MSM was also calculated by the reported method.[44] In our case where peracetic acid was used as an oxidant and Nb/MSM as catalyst, TOF was found to be 163.

Table 2 Catalytic performance of Nb/MS in epoxidation of ethylene

S. no.	Catalyst	TOF	X_{PAA} (%) ($\pm 3\%$)	U_{PAA} (%) ($\pm 3\%$)
1	Nb/MSM	163	14.30	17.21
2	MSM	0	0	0
3	Nb/MSM[a]	0	11.4	0

[a] Blank run was carried out without addition of ethylene keeping other conditions the same as in original experiment.

In comparison, TOF has a value of 89 in a research report by Wu *et al.* where H_2O_2 was used as an oxidant along with Nb/MSM catalyst.[44] Thus, it can be inferred that peracetic acid is more potential oxidant for EO formation as compared to H_2O_2.

Moreover, in order to achieve optimum selectivity of catalyst towards EO production and conversion of ethylene to EO, LPE was carried out at various reaction parameters like temperature, catalyst amount, ethylene to PAA molar ratio, and in the presence of different solvents.

4.1.2 Effect of temperature. We investigated the temperature dependency on the ethylene conversion and selectivity of the catalyst for EO production under three different conditions (50, 60, and 70 °C). The other reaction parameters were kept constant, including ethylene to PAA (32%) 1 : 2 molar ratio and catalyst amount. The reaction was carried out for 6 h using acetonitrile as a solvent and the results of this study are shown in Fig. 5. When the reaction was carried out at 50 °C, the ethylene conversion was 57%, while the selectivity of the catalyst was 90.1%. At 60 °C, ethylene conversion increased from 57 to 73.6%, while selectivity decreased from 90.1% to 83.2%. Similarly at 70 °C, the ethylene conversion showed a slight improvement with a value of 74.8%, but the selectivity of the catalyst was further declined to 79.6%. The decreased selectivity of catalyst towards EO production at elevated temperature can be attributed to the formation of the acetic acid and derivatives

of glycol as by-products. It is well established that this reaction proceeds *via* the formation of ethylene oxide intermediate, and at higher temperature C–C bond is more stable as compared to C–O bond.[45,46] Moreover, the accelerated decomposition of peracetic acid at higher temperatures lead to the enhanced ethylene conversion and decreased catalyst selectivity towards EO production.[47] Thus, it can be inferred that 60 °C is the optimum temperature where highest possible ethylene conversion and catalyst selectivity towards EO production in the presence of Nb/MSM can be achieved.

4.1.3 Effect of catalyst amount. The percentage conversion of ethylene and selectivity towards the EO production significantly depend upon the amount of catalyst. By varying catalyst amounts from 0.1 g to 0.5 g, the reaction was conducted at the optimized temperature of 60 °C and ethylene to oxidant molar ratio of 1 : 2 in acetonitrile solvent for 6 h (Fig. 6). An increase in the catalyst amount resulted in a significant improvement in the ethylene conversion and a marginal enhancement in the selectivity towards the EO production. These results can be interpreted on the basis of an increase in the active species of metal oxide (with increasing catalyst amount), which, in turn, expedited the rate of the reaction. As it is clear from Fig. 6, when the catalyst amount was increased from 0.1 to 0.3 g, the ethylene conversion was remarkably improved from 53.6% to 73.6%. Further increase in catalyst amount resulted in only a small improvement in the ethylene conversion. However, an increase in the catalyst amount from 0.1–0.5 g could only increase the value of selectivity from 82.2–83.9%. Thus, a catalyst amount of 0.3 g can be considered as an optimized catalyst amount under the presented reaction conditions.

4.1.4 Effect of ethylene to PAA molar ratio. The effect of ethylene to PAA molar ratio, on the conversion of ethylene and selectivity of EO, was evaluated by carrying the epoxidation of ethylene under the optimized condition of temperature (60 °C) and catalyst amount (0.3 g) using acetonitrile as solvent. In this
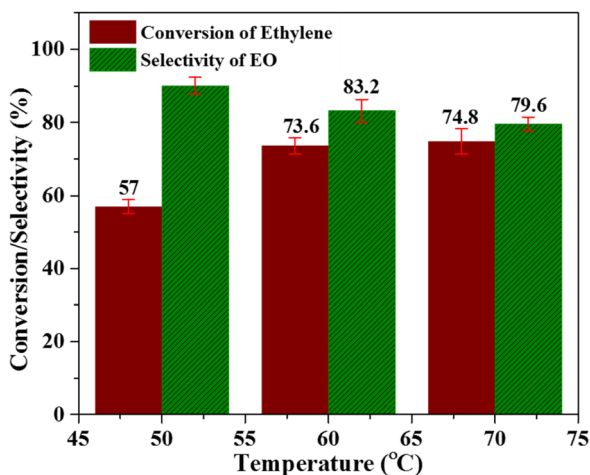

Fig. 5 Effect of temperature [reaction conditions: ethylene = 3.28 mmol (32%) PAA = 6.5 mmol, time = 6 h, catalyst amount = 0.3 g, solvent = C_2H_3N (20 mL)].
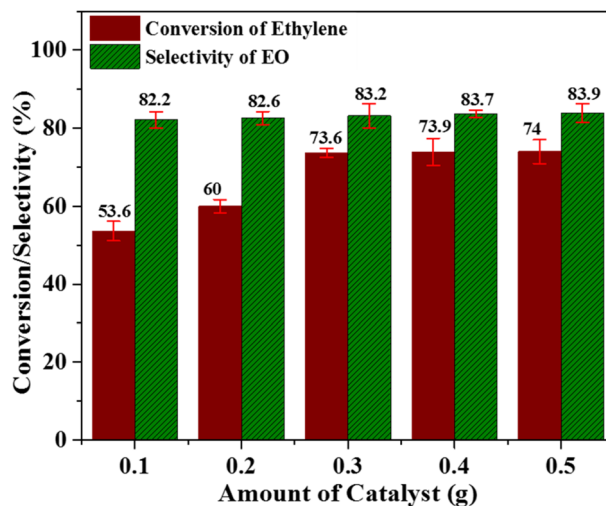

Fig. 6 Effect of catalyst amount; [reaction conditions: ethylene = 3.28 mmol, (32%) PAA = 6.56 mmol, time = 6 h, solvent = C_2H_3N (20 mL), temperature = 60 °C].
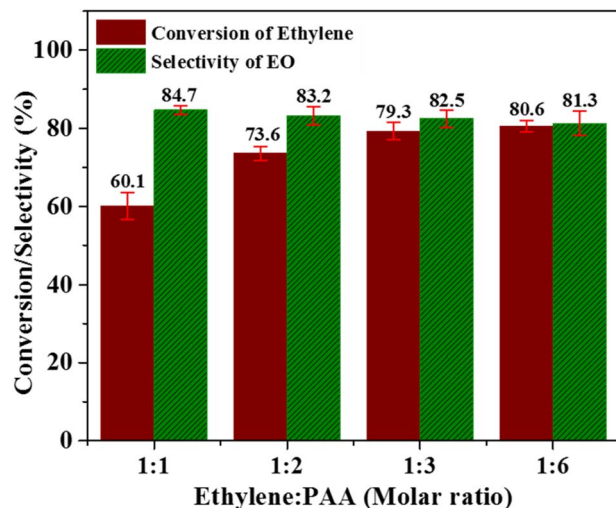
Fig. 7 Effect of ethylene to PPA molar ratio; [reaction conditions: ethylene = 3.28 mmol, catalyst amount = 0.3 g, time = 6 h, solvent = C_2H_3N (20 mL), temperature = 60 °C].

Fig. 8 Effect of several solvents; [reaction conditions: ethylene = 3.28 mmol, (32%) PAA = 8.78 mmol, temperature = 60 °C, time = 6 h, catalyst = 0.3 g, solvent = C_2H_3N (20 mL)].

experiment, various ethylene to PAA molar ratios were used including 1 : 1, 1 : 2, 1 : 3, 1 : 6. As obvious from Fig. 7, the ethylene conversion has a value of 60.1% at the ethylene: PAA molar ratio of 1 : 1. This continuously increased with increasing amount of PAA and reached a maximum value of 80.6% at the molar ratio of 1 : 6. However, the selectivity towards EO production displayed the opposite trend *i.e.* it continuously decreased with increasing amount of PAA. This can be related with pronounced decomposition of PAA at higher concentration instead of its attachment with catalyst active sites. It can be inferred from these results that using excessive amount of the oxidant is not helpful in improving the catalyst activity. Therefore, ethylene to PAA molar ratio of 1 : 3 is the optimum molar ratio where both ethylene conversion and selectivity of EO production are having trade-off values.

4.1.5 Effect of solvent. The solvent effect on the conversion of ethylene and EO production was evaluated using different solvents such as ethyl acetate, acetonitrile, chloroform, and acetone in the presence of Nb/MSM catalyst under optimized reaction conditions of temperature, ethylene to oxidant molar ratio, and amount of catalyst. It was found that acetonitrile solvent proved to be a good solvent for the conversion of ethylene where its value was 79.3%. It is also obvious from Fig. 8 that decrease in solvent polarity has a detrimental effect on the conversion of ethylene, it has the values of 36.5, 21.4, and 15.6% in acetone, ethyl acetate, and carbon tetra chloride respectively. Higher ethylene conversion in more polar solvent can be attributed to promoted mass transfer and uniformity in different phases involved.[45] However, in this study, the selectivity of EO presented a random trend showing that it is not much affected by the solvent change.

From all these studies, it can be concluded that the trade-off conditions for having optimum EO selectivity and ethylene conversion are; temperature (60 °C), catalyst amount (0.3 g), and ethylene : PAA molar ratio (1 : 3). Acetonitrile is the best solvent for EO formation in LPE using Nb/MSM catalyst along with PAA oxidant. To the best of our knowledge no other literature report is available where peracetic acid is used as an oxidant with Nb/MSM catalyst for EO formation.

We speculate that peracetic acid may contribute to hydrolysis of EO which can reduce the EO selectivity. In order to decrease opening of the epoxide ring, epoxidation should be carried out at a possible lower catalyst loading on the support because higher catalyst/acidity in the catalyst can result in increased decomposition of oxidant and more hydrolysis of EO ring.[34] Also it is well reported that water that is produced in the process can increase Brønsted acid sites by blocking Lewis acid sites. These Brønsted acid sites result in increased hydrolysis of epoxide ring.[32] However, it is difficult to manage the water, which is produced in the process. The investigations for reducing the hydrolysis of EO are currently under process.

4.1.6 Leaching property of Nb/MSM catalyst. Nb/MSM metal leaching test was performed by filtering out the catalyst from the hot reaction mixture at 60 °C after 6 hours, and the supernatant reaction mixture was allowed to proceed for another 6 hours making a total reaction time of 12 hours.

Both the samples, collected at 6 hours and 12 hours, were analysed by GC technique to assess any further conversion of ethylene. The analysis revealed no further conversion of ethylene as shown in Fig. 9. This data demonstrates well that Nb/MSM heterocatalyst (when used with peracetic acid oxidant) is also very effective in alleviating the problem of leaching encountered in case of other metal based catalysts used for EO production.

This leaching resistance/no epoxidation due to some leached species (if any) can be explained according to reported literature.[48] In the epoxidation process oligomerized metal oxide species are produced on the surface of the catalyst in the presence of oxidant. According to Das *et al.*, these oligomerized metal oxide species cannot catalyze the epoxidation process.[48] We assume that such oligomerized metal oxide can also be

Nb	Niobium
W	Tungsten
PAA	Peracetic acid
NbCl$_5$	Niobium(v) chloride
SiO$_2$	Mesoporous silicate
TEOS	Tetraethylorthosilicate
EG	Ethylene glycol
AA	Acetic acid
XRD	X-ray diffraction
BET	Brunauer–Emmett–Teller
TEM	Transmission electron microscope
GC	Gas chromatography
P123	Pluronic
ACN	Acetonitrile (C_2H_3N)
AA	CH_3COOH
EO	C_2H_4O
MEG	$C_2H_6O_2$
DEG	$C_6H_{10}O_4$
PAA	CH_3COOOH
BJH	Barrett–Joyner–Halenda
S_{BET}	Surface area
V_{BJH}	Cumulative pore volume
D_{BJH}	Mesoporous diameter
RT	Retention time

Fig. 9 Leaching test for Nb/MSM catalyst for conversion of ethylene.

present in the supernatant solution which was collected for the leaching test. The investigation of the nature of the metal species (if present in supernatant) are outside the scope of the presented study, however, these investigations are being carried out separately.

5. Conclusions

An environmentally friendly production of EO was achieved by the preparation of Nb/MSM catalyst by liquid phase epoxidation of ethylene. To synthesize the catalyst, niobium oxide was supported on mesoporous silica. By using the XRD technique, the hetero atom structure in Nb/MSM was confirmed, and N$_2$ adsorption isotherms were used to evaluate the mesoporous structure. Catalytic activity of Nb/MSM towards EO production was examined using liquid phase epoxidation of ethylene in the presence of peracetic acid as an oxidant. The 79.3% conversion of ethylene with 82.5% selectivity, towards ethylene oxide, was achieved by Nb/MSM metal catalyst. For this purpose, various reaction conditions were optimized including temperature (60 °C), catalyst dosage (0.3 g), and ethylene to PAA molar ratio (1 : 3), and reaction time (6 h) using acetonitrile as an organic solvent. These investigations and obtained results confirmed that the prepared Nb/MSM is a potential catalyst for an efficient EO production.

Abbreviations

EO	Ethylene oxide
CO$_2$	Carbon dioxide
GPE	Gas phase epoxidation
LPE	Liquid phase epoxidation
MTO	Methyltrioxorhenium
H$_2$O$_2$	Hydrogen peroxide
Re	Rhenium
MSM	Mesoporous silica material
MCM-41	Mobile composition of matter no. 1
SBA-15	Santa Barbara amorphous-15

Author contributions

Conceptualization, Toheed Akhter, Asif Mahmood; methodology, Muhammad Maqbool and Asif Mahmood; validation, Toheed Akhter and Asif Mahmood; formal analysis, Muhammad Maqbool and Toheed Akhter; investigation, Muhammad Maqbool; resources, Sohail Nadeem, Muhammad Faheem and Chan Ho Park; writing—original draft preparation, Toheed Akhter and Muhammad Maqbool; writing—review and editing, Toheed Akhter and Chan Ho Park; supervision, Toheed Akhter and Asif Mahmood; all authors have read and agreed to the published version of the manuscript.

Conflicts of interest

There are no conflicts to declare.

References

1 V. Dal Santo, M. Guidotti, R. Psaro, L. Marchese, F. Carniato and C. Bisio, *Proc. R. Soc. A*, 2012, **468**, 1904–1926.
2 L. Pinaeva and A. Noskov, *Pet. Chem.*, 2020, **60**, 1191–1206.
3 V. K. Aggarwal, R. S. Grainger, G. K. Newton, P. L. Spargo, A. D. Hobson and H. Adams, *Org. Biomol. Chem.*, 2003, **1**, 1884–1893.
4 H.-J. Lee, M. Ghanta, D. H. Busch and B. Subramaniam, *Chem. Eng. Sci.*, 2010, **65**, 128–134.
5 M. Ghanta, T. Ruddy, D. Fahey, D. Busch and B. Subramaniam, *Ind. Eng. Chem. Res.*, 2013, **52**, 18–29.
6 D. M. Minahan and G. B. Hoflund, *J. Catal.*, 1996, **158**, 109–115.

7 F. Carniato, C. Bisio, E. Boccaleri, M. Guidotti, E. Gavrilova and L. Marchese, *Eur. J. Chem.*, 2008, **14**, 8098–8101.

8 M. Selvaraj, D.-W. Park, I. Kim, S. Kawi and C. Ha, *Dalton Trans.*, 2012, **41**, 9633–9638.

9 M. Selvaraj, M. Kandaswamy, D. Park and C. Ha, *Catalysis*, 2010, **158**, 286–295.

10 M. Selvaraj and P. Sinha, *New J. Chem.*, 2010, **34**, 1921–1929.

11 M. Selvaraj, M. Kandaswamy, D. Park and C. Ha, *Catalysis*, 2010, **158**, 377–384.

12 R. A. Sheldon, M. Wallau, I. Arends and U. Schuchardt, *Acc. Chem. Res.*, 1998, **31**, 485–493.

13 C. Copéret, M. Chabanas, R. Petroff Saint-Arroman and J. M. Basset, *Angew. Chem.*, 2003, **42**, 156–181.

14 J. M. Thomas, *Chem. Phys.*, 2008, **128**, 182502.

15 D. J. Xuereb and R. Raja, *Catal. Sci. Technol.*, 2011, **1**, 517–534.

16 V. Dal Santo, M. Guidotti, R. Psaro, L. Marchese, F. Carniato and C. Bisio, *Proc. R. Soc. A*, 2012, **468**, 1904–1926.

17 Y. Liu, K. Murata and M. Inaba, *Chem. Lett.*, 2003, **32**, 992–993.

18 F. Somma, P. Canton and G. Strukul, *J. Catal.*, 2005, **229**, 490–498.

19 M. Trejda, A. Tuel, J. Kujawa, B. Kilos and M. Ziolek, *Microporous Mesoporous Mater.*, 2008, **110**, 271–278.

20 J. V. Coelho, L. C. Oliveira, F. C. Moura, P. P. de Souza, C. A. Silva, K. B. Batista and M. J. da Silva, *Appl. Catal., A*, 2012, **419**, 215–220.

21 A. Feliczak-Guzik, A. Wawrzyńczak and I. Nowak, *Microporous Mesoporous Mater.*, 2015, **202**, 80–89.

22 P. Chagas, H. S. Oliveira, R. Mambrini, M. Le Hyaric, M. V. de Almeida and L. C. Oliveira, *Appl. Catal., A*, 2013, **454**, 88–92.

23 S. L. Barbosa, G. R. Hurtado, S. I. Klein, V. L. Junior, M. J. Dabdoub and C. F. Guimaraes, *Appl. Catal., A*, 2008, **338**, 9–13.

24 V. S. Braga, I. C. Barros, F. A. Garcia, S. C. Dias and J. A. Dias, *Catalysis*, 2008, **133**, 106–112.

25 A. Feliczak-Guzik and I. Nowak, *Catalysis*, 2009, **142**, 288–292.

26 I. Nowak, A. Feliczak, I. Nekoksová and J. Čejka, *Appl. Catal., A*, 2007, **321**, 40–48.

27 F. Quignard, A. Choplin and R. Teissier, *J. Mol. Catal. A: Chem.*, 1997, **120**, L27–L31.

28 E. Gianotti, M. E. Raimondi, L. Marchese, G. Martra, T. Maschmeyer, J. M. Seddon and S. Coluccia, *Catal. Lett.*, 2001, **76**, 21–26.

29 K. Kang and W. Ahn, *J. Mol. Catal. A: Chem.*, 2000, **159**, 403–410.

30 W. Adam, W. Malisch, K. J. Roschmann, C. R. Saha-Möller and W. A. Schenk, *J. Organomet. Chem.*, 2002, **661**, 3–16.

31 A. Held and P. Florczak, *Catalysis*, 2009, **142**, 329–334.

32 W. Yan, A. Ramanathan, M. Ghanta and B. Subramaniam, *Catal. Sci. Technol.*, 2014, **4**, 4433–4439.

33 J. Zhang, Z. Xin, X. Meng, Y. Lv and M. Tao, *Fuel*, 2014, **116**, 25–33.

34 W. Yan, A. Ramanathan, P. D. Patel, S. K. Maiti, B. B. Laird, W. H. Thompson and B. Subramaniam, *J. Catal.*, 2016, **336**, 75–84.

35 S. Linic and M. A. Barteau, *J. Am. Chem. Soc.*, 2003, **125**, 4034–4035.

36 S. Linic and P. Christopher, *ChemCatChem*, 2010, **2**, 1061–1063.

37 X. Zhao, S. Veintemillas-Verdaguer, O. Bomati-Miguel, M. Morales and H. Xu, *Phys. Rev. B: Condens. Matter Mater. Phys.*, 2005, **71**, 024106.

38 D. R. Das and A. K. Talukdar, *ChemistrySelect*, 2017, **2**, 8983–8989.

39 a. C. Kresge, M. Leonowicz, W. J. Roth, J. Vartuli and J. Beck, *Nature*, 1992, **359**, 710–712.

40 J. S. Beck, J. C. Vartuli, W. J. Roth, M. E. Leonowicz, C. Kresge, K. Schmitt, C. Chu, D. H. Olson, E. Sheppard and S. McCullen, *J. Am. Chem. Soc.*, 1992, **114**, 10834–10843.

41 G. Somorjai and R. Rioux, *Catal. Today*, 2005, **100**, 201–215.

42 A. L. Linsebigler, G. Lu and J. T. Yates Jr, *Chem. Rev.*, 1995, **95**, 735–758.

43 B. Kalita, P. Phukan and A. K. Talukdar, *Catal. Sci. Technol.*, 2012, **2**, 2341–2350.

44 X. Lu, W.-J. Zhou, Y. Guan, A. Liebens and P. Wu, *Catal. Sci. Technol.*, 2017, **7**, 2624–2631.

45 S. Narayanan, J. J. Vijaya, S. Sivasanker, C. Ragupathi, T. Sankaranarayanan and L. J. Kennedy, *J. Porous Mater.*, 2016, **23**, 741–752.

46 J. Liu, Z. Wang, P. Jian and R. Jian, *J. Colloid Interface Sci.*, 2018, **517**, 144–154.

47 W. Zhan, Y. Guo, Y. Wang, X. Liu, Y. Guo, Y. Wang, Z. Zhang and G. Lu, *J. Phys. Chem. B*, 2007, **111**, 12103–12110.

48 D. R. Das, P. Kalita and A. K. Talukdar, *J. Porous Mater.*, 2020, **27**, 893–903.